

Structural and electrical characteristics of RF sputtered YON gate dielectrics and their thin-film transistor applications

This article has been downloaded from IOPscience. Please scroll down to see the full text article.

2011 J. Phys. D: Appl. Phys. 44 155403

(<http://iopscience.iop.org/0022-3727/44/15/155403>)

View [the table of contents for this issue](#), or go to the [journal homepage](#) for more

Download details:

IP Address: 130.237.29.138

The article was downloaded on 28/03/2011 at 14:25

Please note that [terms and conditions apply](#).

Structural and electrical characteristics of RF sputtered YON gate dielectrics and their thin-film transistor applications

Zhimin Liu¹, Lingyan Liang¹, Zheng Yu¹, Shikun He², Xiaojuan Ye¹, Xilian Sun¹, Aihua Sun¹ and Hongtao Cao¹

¹ Ningbo Institute of Materials Technology and Engineering (NIMTE), Chinese Academy of Sciences (CAS), Ningbo 315201, People's Republic of China

² National Laboratory for Condensed Matter Physics, and Institute of Physics, Chinese Academy of Sciences (CAS), Beijing 100190, People's Republic of China

E-mail: H.cao@nimte.ac.cn and lly@nimte.ac.cn

Received 20 January 2011, in final form 27 February 2011

Published 28 March 2011

Online at stacks.iop.org/JPhysD/44/155403

Abstract

In this paper, we report on rf sputtered high- k YON gate dielectrics and their application on transparent thin-film transistors (TFTs). The N incorporation into the Y_2O_3 matrix is believed to restrain crystalline growth which enables a low leakage current, but boost ion polarization or/and dipole oscillation which results in dielectric frequency dispersion. After forming gas annealing (FGA) treatment, the detrimental polarization mechanisms responsible for the dielectric frequency dispersion are minimized. As a result, it is found that both the 400 °C FGA treated YON gate dielectrics and the TFTs based on them present competitive electrical properties.

(Some figures in this article are in colour only in the electronic version)

1. Introduction

Transparent electronic circuits are expected to serve as the basis for new electronic and optoelectronic devices [1]. The key procedure to realize transparent circuits is transparent thin-film transistor (TFT). Ever-increasing interest in high permittivity (k) metal oxides for TFT application stems from several potential advantages such as a compensation for the relatively low mobility in the semiconductor channel, a reduction in the operating voltage by increasing the gate capacitance and an increment in the charge density at lower gate potentials [2]. Binary metal oxides, such as Al_2O_3 , Ta_2O_5 , HfO_2 , Y_2O_3 and ZrO_2 , have been intensively studied for that purpose [2, 3]. Among those oxides, Y_2O_3 -based gate dielectric has received considerable attention, because of its high thermodynamic compatibility, wide band gap (5.5–6 eV) and relatively high dielectric constant (14–18) [4, 5]. These properties are desirable for alternative gate dielectric, in that a high band gap can enlarge the conduction band offset between gate dielectric and channel layer so as to suppress the leakage current, while a moderate dielectric constant can yield a small sub-threshold slope and a low threshold voltage.

However, pure Y_2O_3 is easy to convert from amorphous to polycrystalline microstructure during the post-annealing treatment, which leads to high defect density around grain boundaries and unendurable leakage current. N incorporation technology has been intensively investigated in poly-Si/high- k devices [6–8]. Studies revealed that high- k oxides can benefit from N doping due to the enhancement on dielectric capacitance, increase in crystalline temperature and improvement of breakdown characteristics [6–8]. So far, N-doped Y_2O_3 via N_2 plasma or NH_3 -ambient annealing has been reported [9, 10]. However, these methods cause an increase in interface trap density and a degradation of mobility due to their inherently non-uniform nature [11]. In addition, the reported YON films were deposited through the high-temperature route, which cannot be conducted on the ITO substrate and thus limits their application in transparent TFTs.

In this paper, we focus on the structural and electrical characteristics of rf sputtered YON films grown on ITO substrates and their applications on thin film transistors. The fabrication process, featuring low temperature, is compatible with the current semiconductor process. Moreover, the YON dielectric layer shows fairly nice interface compatibility with

$\text{In}_2\text{O}_3\text{-ZnO}$ (IZO) channel and the TFTs based on them present competitive electrical properties, which is useful to further advance transparent electronics.

2. Experiment details

YON and Y_2O_3 (as reference) were deposited on various substrates using conventional radiofrequency magnetron sputtering from a metallic Y (99.9% purity) target at room temperature. The YON sputtering was performed in $\text{Ar}/\text{N}_2\text{O}$ ambient while Y_2O_3 was in Ar/O_2 . The discharge power density was 4 W cm^{-2} and working pressure was 30 mTorr. After deposition, forming gas annealing (FGA) treatment was performed in a N_2/H_2 (95% N_2 and 5% H_2) ambient at 200–400 °C for 10 min. X-ray diffraction (XRD) patterns were recorded in θ - 2θ mode by a multipurpose x-ray diffractometer (Bruker, D8 Advance) working with $\text{Cu-K}\alpha$ radiation. The phase composition of the YON thin films was analysed on an Axis Ultra X-ray photoelectron spectroscopy (XPS, Kratos Analytical Ltd, UK) equipped with a standard monochromatic $\text{Al-K}\alpha$ source ($h\nu = 1486.6\text{ eV}$). High dose of argon ions was used to sputter away the top hydrated and carbon contamination layer (2–3 nm) of the films. The binding energy data were calibrated with respect to the C1s signal of ambient hydrocarbons (C–H and C–C) at 284.8 eV.

Capacitance–voltage (C–V) data of Au-Ti/YON/ITO capacitors were measured at various frequencies using a parameter analyser and capacitance–voltage meter (Agilent 4284). The area of each Ti/Au electrode was about $3 \times 10^{-4}\text{ cm}^2$. In addition, IZO-based TFTs applying the fabricated YON films as gate dielectric were also manufactured. The deposition process of the IZO channel was described elsewhere in detail [12]. The thickness of the channel and gate dielectric layers was approximately 80 nm and 420 nm, respectively. The length (L) and width (W) of the channels were 200 μm and 1600 μm , respectively. The electrical characteristics of the TFTs were measured with a precision semiconductor analyser (Keithley 4200) in the dark at room temperature.

3. Results and discussion

Figure 1 gives the XPS spectra of the as-deposited and 400 °C FGA-treated YON films and the as-deposited Y_2O_3 film (as the reference), respectively. The Y_2O_3 reference film shows a peak at 529.1 eV related to the O–Y bond in the O 1s spectrum, a doublet corresponding to the $3d_{5/2}$ and $3d_{3/2}$ features of Y_2O_3 at 156.6 and 158.6 eV in the Y 3d spectrum and a peak at 394.5 eV in the Y 3s spectrum [13].

The XPS spectra of the YON films, however, show very different structures. The N1s/Y3s spectra of the YON films show two features. In addition to the Y 3s peak, there is a broad peak at 399.5 eV related to N 1s (figure 1(c)). It is difficult to assign this peak precisely according to [9, 14], in which the N 1s binding energy of the Y–N, H–N and O–N bonds are reported around 396.2 eV, 401.5 eV and 402 eV, respectively. However, similar to the case of the TiON [14], it is speculated that N has two sites in the YON, one is the crystal lattice interstice of Y_2O_3

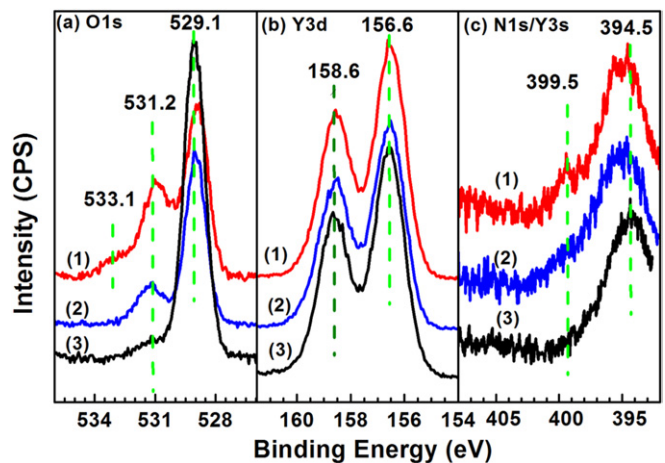


Figure 1. XPS spectra of (a) O1s, (b) Y3d, (c) N1s/Y 3s regions for YON and Y_2O_3 films: (1) As-deposited YON, (2) FGA treated YON, (3) Y_2O_3 reference.

(expressed as the Y–N–O bond) and the other the substitutional site of O (expressed as the Y–N–Y bond), and the N 1s binding energy of the former site is about 2 eV higher than that of the latter due to more negative charge of N residing in the latter site. In fact, the broad peak related to N 1s of the YON films can be deconvoluted into two components at 397.2 eV and 399.7 eV (not show here), which are consistent with the Y–N–Y and Y–N–O bonds, respectively. The incorporation of N in Y_2O_3 also results in a small shift to lower binding energy of the $3d_{5/2}$ and $3d_{3/2}$ peaks in the Y 3d spectra due to the fact that Y has less positive charge in the N–Y bond than in the O–Y bond (figure 1(b)). The O1s spectra of the YON films also display a new obvious feature at 531.2 eV, and the peak related to the Y–O bond shifts to lower binding energy compared with the Y_2O_3 reference because O has more negative charge in the N–Y–O bond than in the O–Y–O bond (figure 1(a)). The O 1s peak at 531.2 eV of the as-deposited YON film is believed to come from the Y–O–H (530.6 eV in [13]) and Y–O–N (532 eV in [15]) bonds, along with a weak peak at 533.1 eV that can be assigned to the absorbed water [13]. Upon the FGA treatment for the YON film, the release of N and OH from the film is supposed to happen, which is supported by the fact that both the N 1s peak and O 1s peak at 531.2 eV get attenuated, the O 1s peak at 531.2 eV shifts to higher binding energy (because of the quick release of OH compared with N), and the feature at 533.1 eV disappears.

In order to investigate the crystallinity, XRD analyses were performed for the as-deposited and 400 °C-annealed YON films, using an as-deposited Y_2O_3 as the reference. As shown in figure 2, three diffraction peaks which correspond to cubic ($Ia\bar{3}$ space group, JCPDS card 25-1200) and monoclinic ($C2/m$ space group, JCPDS card 44-0399) phases of Y_2O_3 reveal the polycrystalline nature of the as-deposited Y_2O_3 film, while the diffraction peaks are almost indistinguishable for the as-deposited YON film and relatively weak for the annealed YON film. Hence, the incorporation of N into Y_2O_3 resulted in a notable increase in the crystalline temperature. A similar result has been reported previously on other materials, such as HfO_2 [11] and ZrO_2 [16].

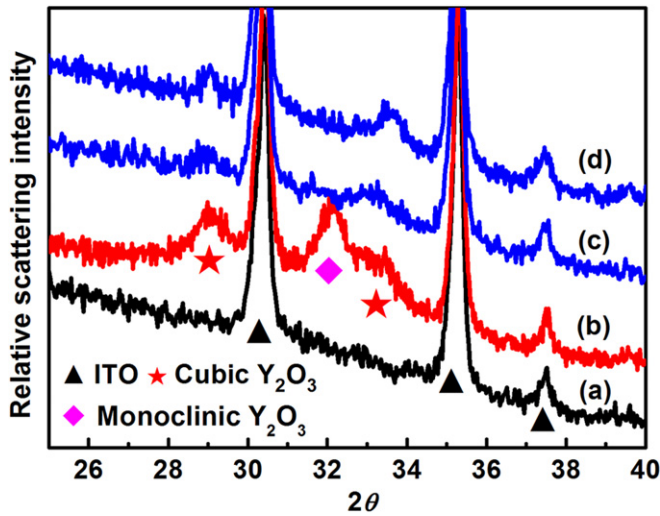


Figure 2. XRD diagrams for (a) ITO substrate, (b) Y_2O_3 reference, (c) As-deposited YON film, (d) 400 °C FGA treated YON film.

Figure 3(a) shows the dependence of dielectric constant (κ) on the frequency of applied electric field. The k is extracted from $C-V$ data using $\kappa = Cd/\epsilon_0A$, where A is the area of the capacitor and d is the dielectric thickness [2]. In comparison with Y_2O_3 , the as-deposited YON film shows higher dielectric constant in response to diverse frequencies, which can be attributed to the N incorporation related charge polarization and ion polarization, similar to the case of HfSiON [6], HfON [8, 17]. Moreover, the as-deposited YON film also displays the obvious frequency dispersion effect of the dielectric constant, which is thought to be caused by the $-ON$ bond induced dipole oscillation, since the frequency dispersion for Y_2O_3 is relatively weaker. Nevertheless, the dependence of the dielectric constant of YON films on frequency becomes weakened after the FGA treatment, which can be related to the decrease in N content, as supported by the XPS result. The leakage current of the YON film after 400 °C FGA treatment ($\sim 0.7 \text{ nA cm}^{-2}$ at 1 MV cm^{-1}) decreases by nearly 3 orders of magnitude compared with the as-deposited one (figure 3(b)), while no obvious reduction in the leakage current is observed for the Y_2O_3 films after the FGA treatment (the inset of figure 3(b)), which is attributed to the polycrystalline nature of the fabricated Y_2O_3 films.

Figure 4(a) shows the schematic of the IZO-TFT with YON as the gate dielectric. As the opaque metal source/drain electrodes were used, the transmittance of the whole device is not displayed herein. However, the YON/ITO/Glass bi-layer has a good transparency with an average transmittance over 80% in the visible spectral region (figure 4(b)). Figures 4(c)–(d) depict the static output and transfer characteristics of the IZO transistor using 400 °C FGA treated YON as the gate dielectric. It is found that the device operates in enhancement mode with features of clear pinch-off and current saturation. The saturation mobility (μ_{sat}) and threshold voltage (V_{TH}), obtained from plotting the square root of the saturation drain current versus gate voltage (V_{GS}), were $26.6 \text{ cm}^2 \text{ V}^{-1} \text{ s}^{-1}$ and 1.8 V, respectively. The on/off ratio and sub-threshold slope (SS) were calculated to be 2.1×10^7 and 0.406 V/decade,

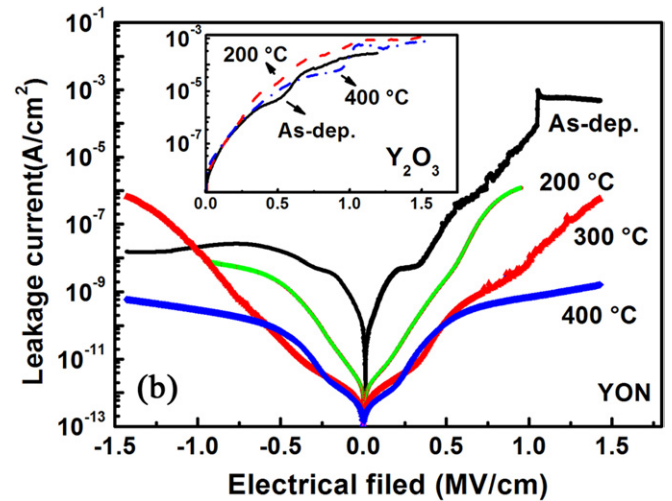
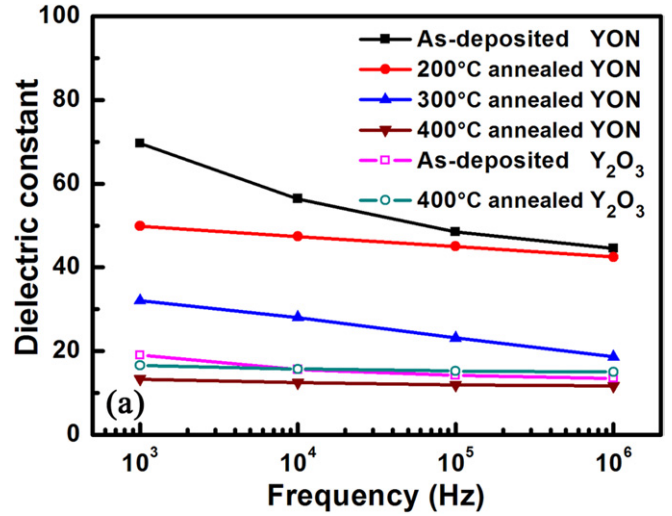


Figure 3. (a) Dielectric constant as a function of frequency, (b) leakage current of as-deposited and FGA treated YON films. The inset plots the leakage current of as-deposited and FGA treated Y_2O_3 films.

respectively. The interface trap density N_t can be deduced from SS using the following expression [18]:

$$N_t = \left(\frac{\log(e)SS}{kT/q} - 1 \right) \frac{C_{\text{ox}}}{q}, \quad (1)$$

where k is Boltzmann's constant, T the absolute temperature, q the electron charge and C_{ox} the capacitance of the gate dielectrics (herein, 24.7 nF cm^{-2} for the 400 °C annealed YON). The calculated N_t is around $8.96 \times 10^{11} \text{ cm}^{-2}$ which is smaller than other dielectric-gated TFTs [18, 19].

4. Conclusions

In summary, the structural and electrical properties of high- k YON dielectrics and their application in thin film transistor were explored. XPS and XRD results show that the N in Y_2O_3 might occupy the substitutional site of O atom or vacancy in the film and simultaneously restrain the crystallization of the film. The as-deposited YON film displays a giant dielectric constant and obvious frequency dispersion behaviour, which

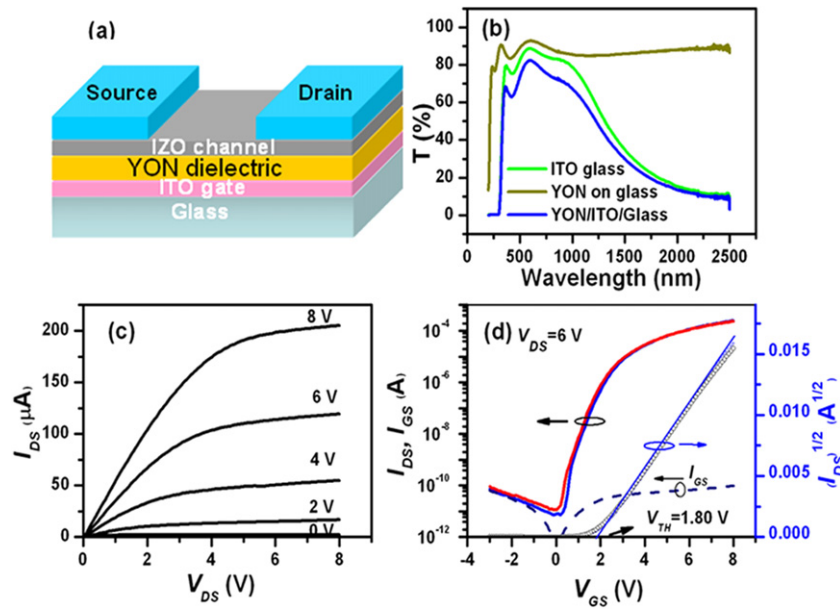


Figure 4. The schematic, optical and electrical characteristics of IZO/YON-based TFTs. (a) The schematic of the thin-film transistors. (b) Optical transmittance of YON film on glass, ITO glass and YON/ITO/glass bi-layers. (c) Output curves of the device. (d) Transfer curve for gate sweep from -3 to 8 V back to -3 V. Drain voltage was 6 V. Field-effect mobility and threshold voltage were determined from the slope of $I_D^{1/2}$ (right-hand ordinate in graph) versus V_{GS} .

can be contributed to the ion polarization and $-ON$ bond induced dipole. After 400°C FGA treatment, the dielectric constant tends to be constant, the leakage current decreases by nearly 3 orders of magnitude, and the average transmittance during the visible region is over 80%. The TFT based on 400°C FGA-treated YON gate dielectric exhibits a field-effect mobility of $26.6\text{ cm}^2\text{ V}^{-1}\text{ s}^{-1}$, an on/off ratio of 2.1×10^7 , a SS of 0.406 V/decade and a threshold voltage of 1.8 V , respectively. All these results suggest that the YON dielectric would be one of the good dielectric candidates for transparent electronics.

Acknowledgments

The authors are grateful for the financial support of the National Natural Science Foundation of China (Grant No 61076081), the Natural Science Foundation of Ningbo (Grant No 2010A610182), the key project of the Natural Science Foundation of Zhejiang province (Grant No Z4080347), the CAS/SAFEA International Partnership Program for Creative Research Teams, the aided program for Science and Technology Innovative Research Team of Ningbo Municipality (2009B21005), and the Special Foundation of President of the Chinese Academy of Sciences (Grand No 080421WA01).

References

- [1] Wager J F 2003 *Science* **300** 1245
- [2] Ahn B D, Kim J H, Kang H S, Lee C H, Oh S H, Kim G H, Li D H and Lee S Y 2006 *Mater. Sci. Semicond. Process.* **9** 1119
- [3] Chen A H, Liang L Y, Zhang H Z, Liu Z M, Ye X J, Yu Z. and Cao H T 2011 *Electrochem. Solid-State Lett.* **14** H88
- [4] Lee Y J, Lee W C, Nieh C W, Yang Z K, Kortan A R, Hong M, Kwo J and Hsu C H 2008 *J. Vac. Sci. Technol. B* **26** 1124
- [5] Evangelou E K, Wiemer C, Fanciulli M, Sethu M and Cranton W 2003 *J. Appl. Phys.* **94** 318
- [6] Koyama M, Kaneko A, Ino T, Koike M, Kamata Y, Iijima R, Kamimuta Y, Takashima A, Suzuki M, Hongo C, Inumiya S, Takayanagi M and Nishiyama A 2002 *Tech. Dig. Int. Electron Devices Meeting IEDM'02* **2002** 849
- [7] Choi C H, Rhee S J, Jeon T S, Lu N, Sim J H, Clark R, Niwa M and Kwong D L 2002 *Tech. Dig. Int. Electron Devices Meeting IEDM'02* **2002** 857
- [8] Kang C S, Cho H J, Choi R, Kim Y H, Kang C Y, Rhee S J, Choi C W, Akbar M S and Lee J C 2004 *IEEE Trans. Electron Devices* **51** 220
- [9] Niu D, Ashcraft R W, Hinkle C and Parsons G N 2004 *J. Vac. Sci. Technol. A* **22** 445
- [10] Wang X J, Zhang L D, He G, Zhang J P, Liu M and Zhu L Q 2008 *Appl. Phys. Lett.* **92** 042905
- [11] Seong N J, Lee W J and Yoon S G 2006 *J. Vac. Sci. Technol. B* **24** 312
- [12] Chen A H, Cao H T, Zhang H Z, Liang L Y, Liu Z M, Yu Z and Wan Q 2010 *Microelectron. Eng.* **87** 2019
- [13] Barve S A, Jagannath, Mithal N, Deo M N, Chand N, Bhanage B M, Gantayet L M and Patil D S 2010 *Surf. Coat. Technol.* **204** 3167
- [14] Zhou Z H and Huang Y 2009 *J. Phys.: Conf. Ser.* **188** 012033
- [15] Zhang H Z, Guo X G, Zhang Q H, Ma Y B, Zhou H C, Li J, Wang L G and Deng Y Q 2008 *J. Mol. Catal. A: Chem.* **296** 36
- [16] Nieh R E, Kang C S, Cho H J, Onishi K, Choi R, Krishnan S, Han J H, Kim Y H, Akbar M S and Lee J C 2003 *IEEE Trans. Electron Devices* **50** 333
- [17] Ino T, Kamimuta Y, Suzuki M, Koyama M and Nishiyama A 2006 *J. Appl. Phys.* **45** 2908
- [18] Cross R B M, De Souza M M, Deane S C and Young N D 2008 *IEEE Trans. Electron Devices* **55** 1109
- [19] Zhang L, Li J, Zhang X W, Jiang X Y and Zhang Z L 2009 *Appl. Phys. Lett.* **95** 072112